Metallurgical and Materials Engineering *Research paper*
Association of Metallurgical Engineers of Serbia AMES *https://doi.org/10.30544/561*

EFFECT OF CHEMICAL COMPOSITION ON THE MICROSTRUCTURE, HARDNESS AND ELECTRICAL CONDUCTIVITY PROFILES OF THE Bi-Ge-In ALLOYS

Aleksandar Đorđević[1], Milena Premović[1], Duško Minić[1], Milan Kolarević[2], Milica Tomović[1]*

[1]University of Priština, Faculty of Technical Science, Kneza Miloša 7, 38220 Kos. Mitrovica, Serbia
[2]University of Kragujevac, Faculty of Mechanical and Civil Engineering in Kraljevo, Kraljevo, Serbia

Received 11.09.2020
Accepted 25.12.2020

Abstract

In this study, the microstructure, hardness, and electrical properties of selected ternary Bi-Ge-In alloys were investigated. Isothermal sections of the Bi-Ge-In system at 25, 200, and 300 °C were extrapolated using optimized thermodynamic parameters from the literature. The used experimental techniques include optical microscopy, X-ray powder diffraction (XRD), scanning electron microscopy (SEM) and energy dispersion spectrometry (EDS), Brinell hardness, and electrical conductivity measurements. The results of EDS phase composition analysis were compared with the calculated isothermal sections and a good overall agreement was reached. The results of the XRD were also in line with the predicted phase balance. By using ANOVA analysis and experimental results of Brinell hardness and electrical conductivity, a mathematical model was suggested for the calculation of these properties along with all composition ranges. The appropriated mathematical model was subsequently used for the prediction of hardness and electrical conductivity throughout the whole composition range.

Keywords: phase equilibrium, mathematical model, hardness, electrical conductivity.

Introduction

The ternary Bi-Ge-In system has been previously investigated by our group [1]. In our previous study, a reliable thermodynamic data set was proposed and experimentally confirmed. For Bi-Ge-In system, three vertical sections Bi-GeIn, Ge-BiIn, and In-BiGe and three isothermal sections at 50, 75, and 100 °C were experimentally investigated [1].

*Corresponding author: Milena Premović, *milena.premovic@gmail.com*

The same thermodynamic parameters obtained in a previous study [1] were used in the current study as well as Pandat software [2].

Both Bi-Ge and Ge-In based alloys have applications in the industry for making different optical and electronic devices [3-5]. Germanium-based alloys have special applications in modern technology for making optical discs, blu-ray discs, flash memory, etc. [6-8]. A very limited number of studies carried out on Bi-Ge-X alloy systems is available in the literature. *Premović et al.* [9] experimentally investigated phase equilibria of the ternary Bi-Ge-Sb system. The phase diagram of the ternary Bi-Ge-Ag system has been experimentally examined and calculated by *Milisavljević et al.* [10]. The main motivation for studying these alloys is to contribute to the further development of their field of application. The results presented in this study should benefit the industry for the development of new alloys. On the other hand, Bi-In alloys are also interesting due to the application as thermoelectric materials [11], multicomponent lead-free solders [12, 13], etc. A large number of ternary systems based on Bi-In are tested but not in combination with Ge. So this is another reason for this work.

Experimental work

In this study, three isothermal sections at 25, 200, and 300 °C were calculated. Thermodynamic calculations of isothermal sections were performed by using Pandat software [2]. Experimental results were obtained using scanning electron microscopy (SEM) with energy dispersive spectrometry (EDS), X-ray powder diffraction (XRD) analysis and inverted metallographic microscope. In addition, important properties such as hardness and electrical conductivity were measured.

High-purity (99.999 wt. %) Bi, Ge, and In metals produced by Alfa Aesar (Germany) were used for the preparation of investigated alloy samples. Three series of samples were prepared i.e., 22 alloys in total. Five of the prepared samples were used for the assessment of phase equilibria at 200 °C and another five for the assessment of phase equilibria at 300 °C. Nominal compositions of the samples were randomly selected. The total mass of each sample was 4 g. Weighed masses of the samples were arc-melted and re-melted five times under a high purity argon atmosphere using a non-consumable tungsten electrode with an average weight loss of around 1 mass %. After melting, three series of samples were prepared (first series annealed at 200 °C, second series annealed at 300 °C, and third series for electrical conductivity and hardness measurements). Samples for investigation of isothermal sections at 200 °C and 300 °C were sealed in evacuated quartz tubes and kept at 200 °C for four weeks and six weeks at 300 °C. After annealing the samples were quenched in the water and ice mixture. These samples were prepared and used for SEM-EDS and XRD analysis.

The compositions of the alloy samples were determined using a JEOL JSM-6460 scanning electron microscope (SEM) and TESCAN VEGA3 scanning electron microscope, which were both equipped with an EDS system (Oxford Instruments X-act). The samples for SEM-EDS analysis were prepared by standard procedure.

Powder XRD data were recorded with a D2 PHASER in the 2θ range from 10° to 75° with a step size of 0.02°.

The last prepared group of the samples was used for light optical microscopy, XRD analysis, electrical conductivity, and hardness measurements. These samples were again melted in an electric furnace under a high-purity argon atmosphere and slowly cooled to

room temperature using a cooling rate of 2 °Cmin^{-1} in a way to achieve equilibrium at room temperature for the hardness and electrical conductivity measurements. The obtained microstructures were inspected using XRD analysis. By using OLYMPUS GX41 optical images of the microstructures were recorded. The samples were prepared by the classic metallographic procedure. INNOVATEST and SIGMATEST 2.069 eddy instruments were used for Brinell hardness and Electrical conductivity measurements, respectively. For the Brinell hardness test, a steel ball with a diameter of 1 mm was used, and a load force of 294.2 N was applied for 20 seconds.

Results and discussion

Constitutive binary systems of the ternary Bi-Ge-In system were extensively studied in the past. Reliable thermodynamic datasets for these binary systems are available in the literature [14-16]. Based on the literature information for binary sub-systems, considered phases, their crystallographic data, and database names (for the solid phases) are summarized in Table 1.

Table 1. Considered phase, their crystallographic data and database names for the solid phases of the ternary Bi-Ge-In system [14-16].

Thermodynamic database name	Common name	Space group symbol	Structural designation	Pearson's symbol
LIQUID	Liquid	-	-	-
RHOMBO_A7	(Bi)	$R\bar{3}mH$	*A7*	*hR2*
DIAMOND_A4	(Ge)	$Fm\bar{3}m$	*A4*	*cF8*
TETRAG_A6	(In)	*I4/mmm*	*A6*	*tI2*
BIIN	BiIn	*P4/nmms*	*B10*	*tP4*
BI3IN5	Bi_3In_5	*I4/mcm*	$D8_1$	*tI32*
BIIN_BRASS	$BiIn_2$	$P6_3/mmc$	$B8_2$	*hP6*
TET_ALPHA1	ε	*I4/mmm*	*A6mod*	*tI2*

According to the information listed in Table 1, stable phases that should appear in the ternary Bi-Ge-In system include liquid phase, solid solution phases (Bi), (Ge), (In) and ε, and three binary intermetallic compounds BiIn, Bi_3In_5 and $BiIn_2$.

Ternary Bi-Ge-In system

Isothermal section at 200 °C

Five ternary samples were annealed at 200 °C for four weeks and then analyzed by using SEM-EDS and XRD techniques. The obtained results are summarized in Table 2.

Table 2. Combined results of SEM-EDS and XRD analyzes of the selected Bi-Ge-In alloys annealed at T=200 °C.

N.	Composition of samples (at. %)	Determined phases		Compositions of phases (at. %)			Lattice parameters (Å)	
		EDS	XRD	Bi	Ge	In	*a=b*	*c*
1.	9.36 Bi 51.42 Ge 39.22 In	L (Ge)	 (Ge)	73.55±0.4 0.83±0.1	1.42±0.5 98.45±0.3	25.03±0.8 0.72±0.9	 5.6557±0.0004	
2.	23.69 Bi 53.21 Ge 23.10 In	L (Ge)	 (Ge)	81.38±0.8 0.14±0.2	1.18±0.1 99.05±0.2	17.44±0.2 0.81±0.2	 5.6585±0.0006	
3.	26.84 Bi 17.93 Ge 55.23 In	L (Ge)	 (Ge)	87.91±0.6 0.67±0.7	0.88±0.3 98.71±0.5	11.21±0.4 0.62±0.2	 5.6456±0.0003	
4.	44.35 Bi 49.17 Ge 6.48 In	L (Ge) (Bi)	 (Ge) (Bi)	69.32±0.8 0.50±0.4 98.18±0.3	3.18±0.1 98.28±0.1 0.98±0.8	27.50±0.2 1.22±0.8 0.84±0.6	 5.6578±0.0001 4.5565±0.0004	 11.8143 ±0.0004
5.	70.18 Bi 10.85 Ge 18.97 In	L (Ge) (Bi)	 (Ge) (Bi)	71.98±0.4 1.26±0.4 97.87±0.7	2.36±0.9 98.25±0.6 1.23±0.3	25.66±0.4 0.49±0.9 0.90±0.7	 5.6821±0.0009 4.5378±0.0002	 11.8345 ±0.0006

Within the five investigated samples, two different phase regions were detected. One is L+(Ge) two-phase region and one is L+(Ge)+(Bi) three-phase region. Samples 1, 2 and 3 belong to the L+(Ge) phase region while samples 4 and 5 to the L+(Ge)+(Bi) phase region. As in samples 1-5, the content of the bismuth increases, from 9.36 at.% (sample 1) to 70.18 at.% (sample 5); this leads to the microstructural changes and appearance of (Bi) solid solution in samples rich with Bi. In all the samples L phase is stable, as well as the (Ge) solid solution. Nonetheless, the stability of (Bi) solid solution changes. So, in samples 4 and 5, (Bi) solid solution is stable. Determined lattice parameters of the (Ge) and (Bi) solid solutions are compared with literature values [17, 18].

SEM micrographs of microstructures of the two samples annealed at 200 °C are presented in Figure 1 as an illustration.

Phases detected by EDS and XRD analysis are marked on the given micrographs. The microstructure of sample 3 consists of two phases: L as a gray phase and (Ge) solid solution as a dark phase. Sample 5 contains three phases in microstructure: L as a gray phase, (Ge) solid solution as a dark phase and solid solution (Bi) as a dark gray phase.

Figure 2 shows a comparison of EDS results summarized in Table 2 and a calculated isothermal section at 200 °C. The obtained experimental results are marked with the same symbol but in a different color to distinguish the results of different samples.

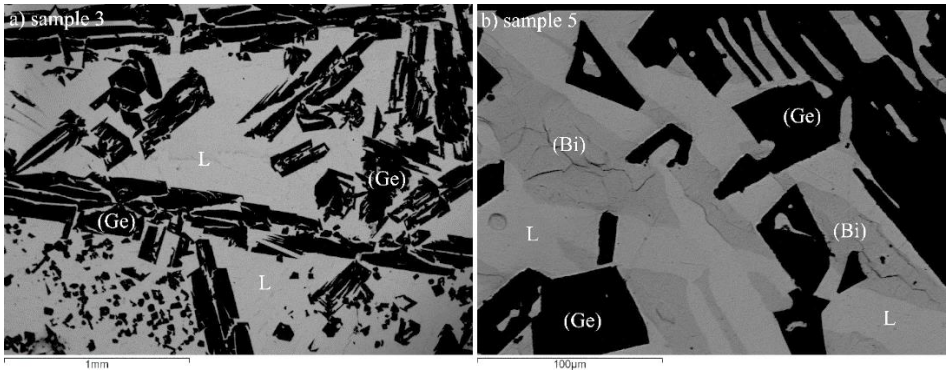

Fig. 1. SEM micrographs of the samples annealed at 200 ºC a) sample 3 and b) sample 5.

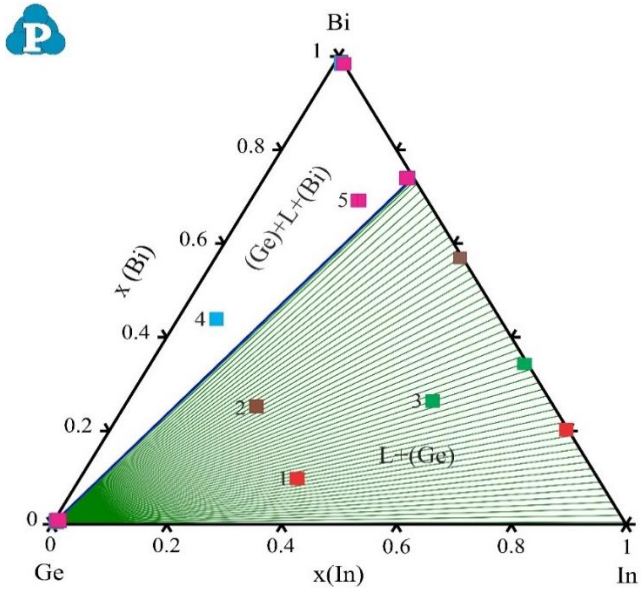

Fig. 2. The calculated isothermal section at 200 °C compared with EDS results given in Table 2.

The calculated isothermal section at 200 °C consists of two different phase regions, one is two phase region L+(Ge) and the other is three phase region (Ge)+L+(Bi). Both were experimentally confirmed by analysis of the samples annealed at 200 °C. Samples 1, 2, and 3 are located in L+(Ge) two-phase region, whereas samples 4 and 5 are located in (Ge)+L+(Bi) three-phase region, in the same phase regions as experimentally proved.

Isothermal section at 300 °C

For the second selected isothermal section of Bi-Ge-In system at 300 °C, five ternary samples annealed at 300 °C were experimentally analyzed and the obtained results (SEM-EDS and XRD) are summarized in Table 3.

Table 3. Combined results of SEM-EDS and XRD analyzes of the selected Bi-Ge-In alloys annealed at T=300 °C.

N.	Composition of samples (at. %)	Determined phases		Compositions of phases (at. %)			Lattice parameters (Å)
		EDS	XRD	Bi	Ge	In	a=b=c
1.	11.41 Bi 65.14 Ge 23.45 In	L (Ge)	(Ge)	56.32±0.4 1.65±0.6	2.76±0.2 97.66±0.1	40.92±0.8 0.69±0.8	5.6556±0.0002
2.	9.65 Bi 39.84 Ge 50.51 In	L (Ge)	(Ge)	66.67±0.6 0.52±0.6	0.83±0.5 98.43±0.3	32.50±0.2 1.05±0.2	5.6512±0.0005
3.	29.96 Bi 17.49 Ge 52.55 In	L (Ge)	(Ge)	45.78±0.1 0.80±0.8	1.24±0.7 99.07±0.3	52.98±0.2 0.13±0.1	5.6435±0.0002
4.	46.45 Bi 40.50 Ge 13.05 In	L (Ge)	(Ge)	72.78±0.6 0.98±0.7	1.65±0.2 98.08±0.1	25.57±0.1 0.94±0.6	5.6587±0.0006
5.	58.81 Bi 10.85 Ge 26.18 In	L (Ge)	(Ge)	83.34±0.7 1.47±0.2	0.78±0.6 97.25±0.6	15.88±0.5 1.28±0.8	5.6556±0.0005

As shown in Table 5, in all tested samples, the same two phases L and (Ge) solid solution were detected. The EDS results show that (Ge) solid solution is expectedly rich with germanium and dissolves a negligible amount of indium and bismuth. L phase is rich in bismuth and indium and dissolves a negligible amount of germanium.

SEM micrograph of the sample annealed at 300 °C is presented in Figure 3.

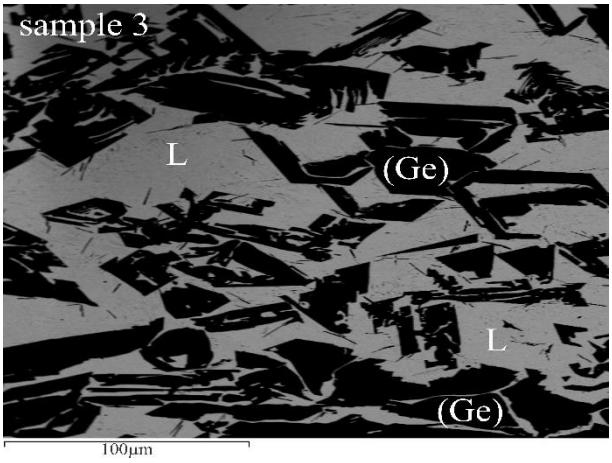

Fig. 3. SEM micrograph of the sample annealed at 300 ºC (sample 3).

Out of the two phases visible in the microstructure of sample 3 (Fig. 3) one is (Ge) solid solution and the other is L phase.

Since the tested samples were annealed at 300 °C, EDS results of the tested samples (Table 3) are compared with a calculated isothermal section at 300 °C. Figure 4, presents the calculated isothermal section at 300 °C compared with the EDS results.

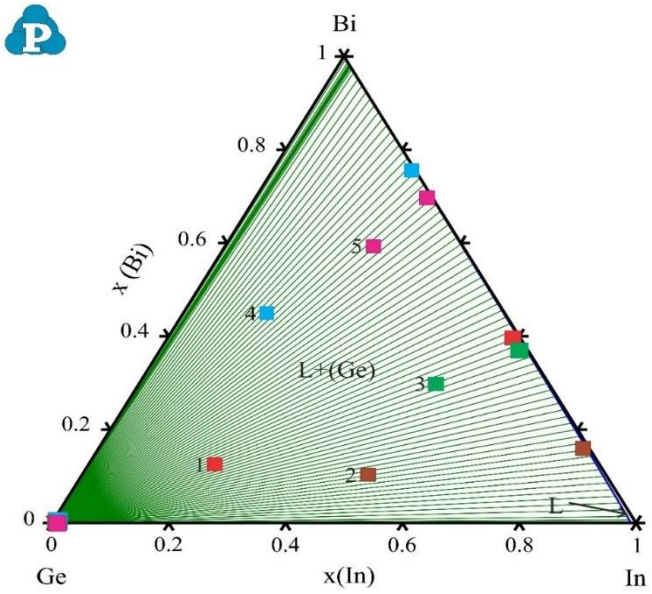

Fig. 4. The calculated isothermal section at 300 °C compared with EDS results given in Table 3.

The calculated isothermal section at 300 °C consists of two phase regions. One is single phase region L and the other is two-phase region L+(Ge). All of the tested samples are located in two-phase region L+(Ge). EDS compositions of the phases are in close agreement with the calculated compositions of the phases.

Microstructural analysis of slowly-cooled samples

Light optical microscope was used for microstructure observations on 12 alloy samples. The samples' compositions are positioned along three vertical sections Bi-GeIn, Ge-BiIn, and In-BiGe. From each section, four samples were prepared and marked with numbers from 1 to 12. The first four samples are from Bi-GeIn section; another four samples are from Ge-BiIn section and the samples marked from 9 to12 are from In-BiGe section. Figure 5 shows compositions of the 12 studied ternary alloy samples and the calculated isothermal section at 25 ºC.

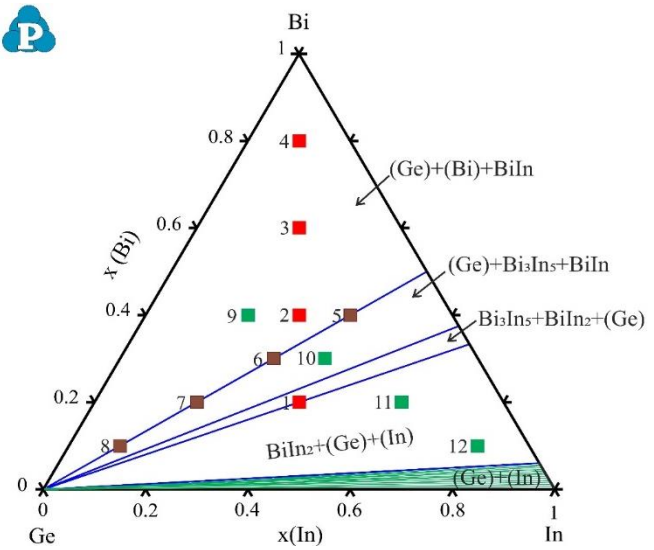

Fig. 5. The predicted isothermal section at 25 ºC and composition of 12 ternary samples.

According to the calculations, sample 1 belongs to the $BiIn_2$+(Ge) region, samples 2-4 and 9 to the (Ge) + (Bi) + BiIn region, samples 5-8 to the (Ge) + BiIn, sample 10 to the (Ge) + Bi_3In_5 + BiIn region, the samples marked with numbers 11 and 12 belong to the $BiIn_2$ + (Ge) + (In) three-phase region. The obtained XRD results support these findings and are in agreement with calculated phase regions.

These samples were used for measurements of mechanical and electrical properties. Two microstructures of samples 2 and 11 are given in Figure 6.

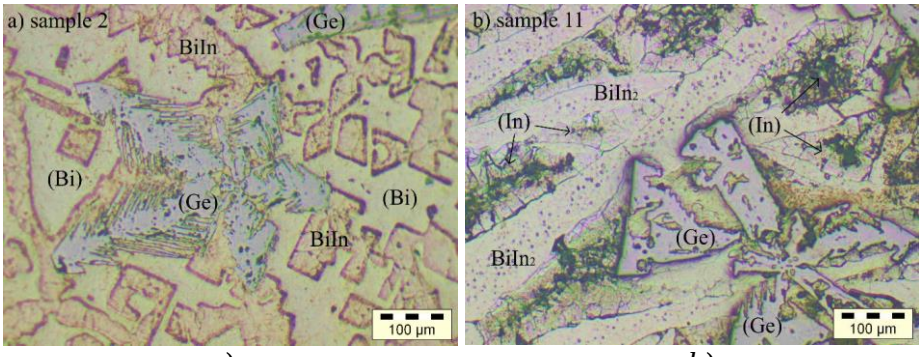

a) *b)*

Fig. 6. LOM micrographs of a) sample 2 and b) sample 11.

Phases that appear in microstructures are marked at presented micrographs.

Brinell hardness measurements

Twelve ternary samples and three binary samples were subjected to the Brinell hardness measurements. Based on the repeated measurements, the mean values of Brinell hardness were calculated and presented in Table 4. Literature values of hardness for pure elements [19] are also shown in Table 4 for comparison.

Table 4. Compositions of the investigated samples at room temperature and measured Brinell hardness values.

N.	Alloy nominal composition (at.%)			Measured value (MN/m^2)			Mean value (MN/m^2)
	x(Bi)	x(Ge)	x(In)	1	2	3	
B1	**0**	0.5	0.5	243.80	249.60	246.30	246.43
1	**0.2**	0.4	0.4	7.30	7.10	7.20	7.20
2	**0.4**	0.3	0.3	8.20	7.30	9.60	8.36
3	**0.6**	0.2	0.2	9.60	10.10	9.30	9.66
4	**0.8**	0.1	0.1	10.40	10.30	10.50	10.40
Bi	**1**	0	0				94.20[19]
B2	0.5	**0**	0.5	93.20	94.10	92.30	93.20
5	0.4	**0.2**	0.4	1.60	1.80	2.30	1.90
6	0.3	**0.4**	0.3	4.80	3.60	3.30	3.90
7	0.2	**0.6**	0.2	4.80	5.30	4.70	4.93
8	0.1	**0.8**	0.1	9.80	10.00	11.60	10.46
Ge	0	**1**	0				973.40[19]
B3	0.5	0.5	**0**	213.20	215.60	217.40	215.40
9	0.4	0.4	**0.2**	9.30	7.80	8.30	8.46
10	0.3	0.3	**0.4**	7.80	4.90	5.60	6.10
11	0.2	0.2	**0.6**	4.90	4.60	4.50	4.66
12	0.1	0.1	**0.8**	4.10	3.80	3.70	3.86
In	0	0	**1**				8.83 [19]

In addition to the tabular presentation, the obtained values for hardness are also presented graphically. Figure 7 shows a graphical representation of the relationship between the hardness and the composition of the tested alloys.

From the obtained results, shown in Table 4, as well as graphically shown in Figure 7 it can be seen that the binary samples $Ge_{50}In_{50}$ and $Bi_{50}Ge_{50}$ have the highest hardness values. Among the other tested ternary samples, the highest hardness value of 10.46 MN/m^2 was recorded for sample 8 ($Bi_{10}Ge_{80}In_{10}$), which is understandable due to the presence of high Ge content in the alloy. In this sample, two phases are stable (Ge)+BiIn; however, the content of (Ge) solid solution phase is much higher than that of BiIn phase. These two phases are also stable in samples 5, 6, and 7 but in a different ratio. Depending on which phase predominates, BiIn or (Ge) hardness is changing. So in sample 5, the dominant phase is BiIn, and in sample 8 dominant phase is (Ge). The lowest value of hardness of 1.90 MN/m^2 was measured for sample 5 ($Bi_{40}Ge_{20}In_{40}$), due to the low content of Ge.

In general, it can be noticed that with an increase of the Bi and Ge content in Bi-Ge-In ternary alloys, the hardness increases. Conversely, an increase of In content in the ternary samples leads to a slight decrease in the hardness.

Response Surface Methodology - RSM was used to quantify the relationship between independent input parameters and the dependent variable (response) [20-24]. Data processing was done in the software package Design Expert v.9.0.6.2. By using the results given in Table 4, a mathematical model for Brinell hardness was developed. Using all possible canonicals or Scheffe models, a Special Cubic model has been suggested. The diagnosis of the statistical properties of the assumed model found that the distribution of residuals is not normal and that it is necessary to transform the mathematical model in order to meet the conditions of normality. The Box-Cox diagnostics recommends the ”Inverse Square Root“ transformation for the variance stabilization.

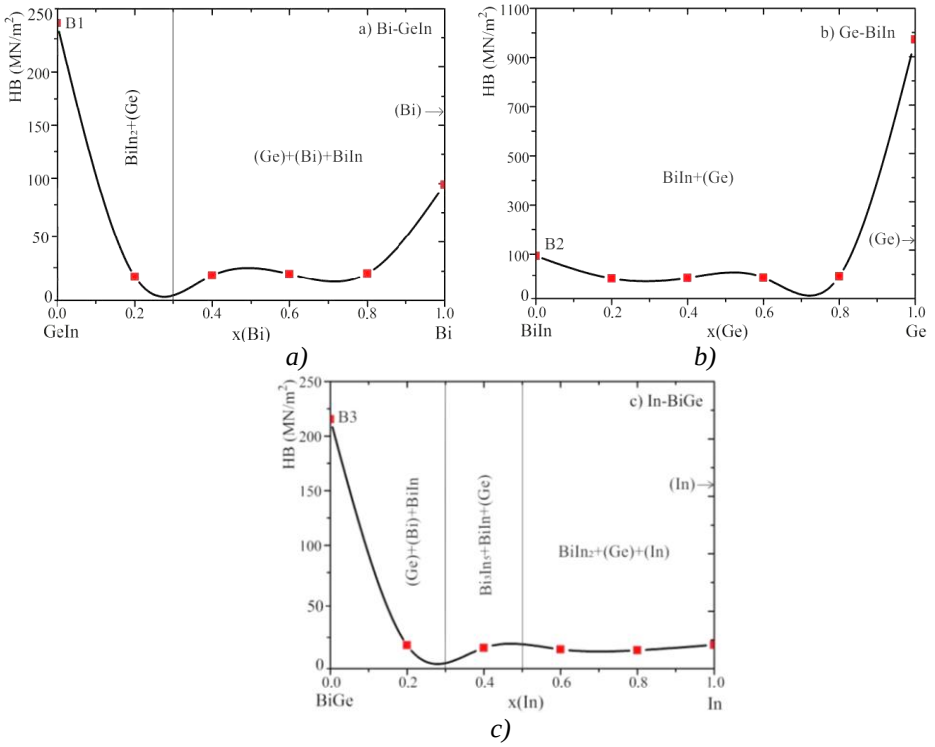

Fig. 7. Graphical presentation of Brinell hardness vs. composition and phase fraction: a) vertical section Bi-GeIn, b) vertical section Ge-BiIn, and c) vertical section In-BiGe.

The final equation of the predictive model in terms of real components is (1):

$$1/Sqrt(HB+1.00) = 0.130602071\cdot(Bi) + 0.102462155\cdot(Ge) + 0.370110518\cdot(In) - 0.05470384\cdot(Bi)\cdot(Ge) - 0.31283672\cdot(Bi)\cdot(In) - 0.44269865\cdot(Ge)\cdot(In) + 9.202504558\cdot(Bi)\cdot(Ge)\cdot(In) \quad (1)$$

The repeated analysis for Inverse Square Root model transformation confirms the significance of the Transformed Special Cubic model. In this case, ANOVA confirms the Reduced Special Cubic Mixture model (Table 5).

Table 5. ANOVA for Special Cubic Mixture model.

Source	Sum of Squares	df	Mean Square	F Value	p-value Prob > F
Model	0.2976	6	0.0496	4.3057	0.0177
Linear Mixture	0.0626	2	0.0313	2.7185	0.1098
AB	0.0001	1	0.0001	0.0115	0.9167
AC	0.0043	1	0.0043	0.3747	0.5529
BC	0.0086	1	0.0086	0.7504	0.4048
ABC	0.1338	1	0.1338	11.6180	0.0058
Residual	0.1267	11	0.0115		
Cor Total	0.4243	17			

The F-value of the Model is 4.30. R-squared and other statistics values are listed in Table 6.

Table 6. R-squared and other statistics after the ANOVA.

Std. Dev.	0.10733	R-Squared	0.70137
Mean	0.29367	Adj R-Squared	0.53847
C.V. %	36.54931	Pred R-Squared	0.36179
PRESS	0.68656	Adeq Precision	5.24704

The diagnosis of the statistics shows that the distribution of residuals is normal. The value of λ is -0.5, the optimum value of λ is -0.37 and the 95% confidence interval for λ (Low C.I.=-0.76, High C.I.=-0.01) contains the value -0.5, thus proving the justification of the model transformation (Figure 8).

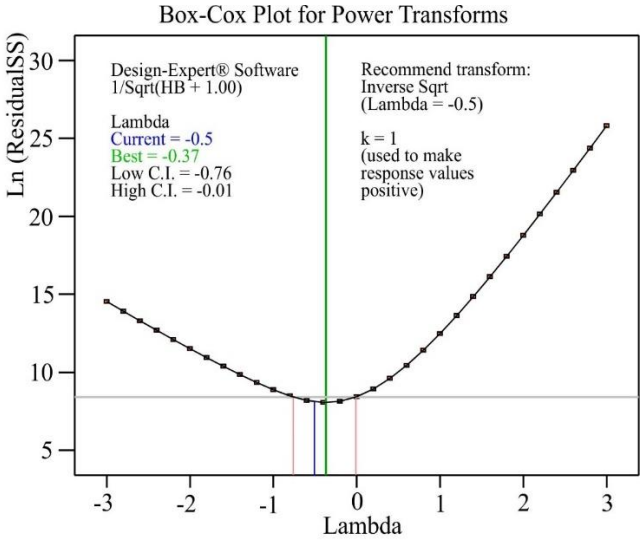

Figure 8. The Box-Cox plot for power transforms.

Figure 9 shows Brinell hardness defined by equation 1.

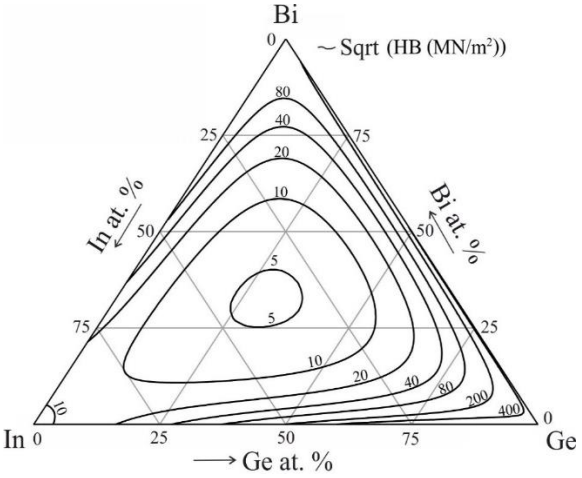

Fig. 9. Calculated iso-lines of Brinell hardness in ternary Bi-Ge-In system with R^2 = 0.701.

Electrical conductivity measurements

Measurements of electrical conductivity were performed on the same group of samples used for the hardness test, and the results are given in Table 7. Besides measured values, Table 7 also includes calculated mean values and literature values of electrical conductivity for pure elements [25].

Table 7. Compositions of the investigated samples at room temperature and the measured electrical conductivity values.

N.	Alloy nominal composition (at.%)			Value (MS /m)				Mean value (MS/m)
	x(Bi)	x(Ge)	x(In)	1	2	3	4	
B1	**0**	0.5	0.5	3.6362	3.8328	3.4332	3.5983	3.6251
1	**0.2**	0.4	0.4	0.3169	0.3200	0.3098	0.3182	0.3162
2	**0.4**	0.3	0.3	0.3233	0.3180	0.3193	0.3158	0.3191
3	**0.6**	0.2	0.2	0.3222	0.3193	0.3281	0.3233	0.3232
4	**0.8**	0.1	0.1	0.3396	0.3289	0.3401	0.3395	0.3370
Bi	**1**	0	0					0.77 [25]
B2	0.5	**0**	0.5	0.2630	0.2840	0.2990	0.2380	0.2710
5	0.4	**0.2**	0.4	0.2935	0.3159	0.3269	0.3278	0.3160
6	0.3	**0.4**	0.3	0.3385	0.3289	0.3258	0.3188	0.3280
7	0.2	**0.6**	0.2	0.3366	0.3419	0.3313	0.3487	0.3396
8	0.1	**0.8**	0.1	0.3596	0.3623	0.3496	0.3554	0.3567
Ge	0	**1**	0					0.002 [25]
B3	0.5	0.5	**0**	0.3430	0.3410	0.3530	0.3440	0.3452
9	0.4	0.4	**0.2**	0.3555	0.4189	0.4266	0.3999	0.4002
10	0.3	0.3	**0.4**	0.6540	0.6799	0.6702	0.6635	0.6669
11	0.2	0.2	**0.6**	0.9630	0.9562	0.9988	1.1023	1.0050
12	0.1	0.1	**0.8**	1.4530	1.6140	1.5030	1.6483	1.5545
In	0	0	**1**					12 [25]

For a more straightforward overview of the results, Figure 10 presents a graphical presentation of the obtained results (mean values) given in Table 7.

It is known that the chemical composition of alloys has a strong influence on electrical conductivity. In the studied ternary Bi-Ge-In alloys, a high value of electrical conductivity was detected in alloys with a high amount of indium. Out of the studied ternary samples, the highest electrical conductivity of 1.5545 MS/m was obtained for $Bi_{10}Ge_{10}In_{80}$ alloy. However, in addition to the composition of the alloy, the phase components and their amount can also significantly affect the electrical conductivity. For example, in samples 11 and 12 the same three phases are in equilibrium $BiIn_2$, (Ge), and (In). In samples 11 and 12, ratios between $BiIn_2$, (Ge), and (In) is different, and this has a direct effect on the electrical conductivity. So in sample 12 where (In) solid solution phase is dominant electrical conductivity is high.

A quadratic Mixture model was suggested as a final equation for the prediction of electrical conductivity. The distribution of residuals is not normal and that it is necessary to transform the mathematical model in order to meet the conditions of normality. The Box-Cox diagnostics recommends the ”Natural Log“ transformation for the variance stabilization.

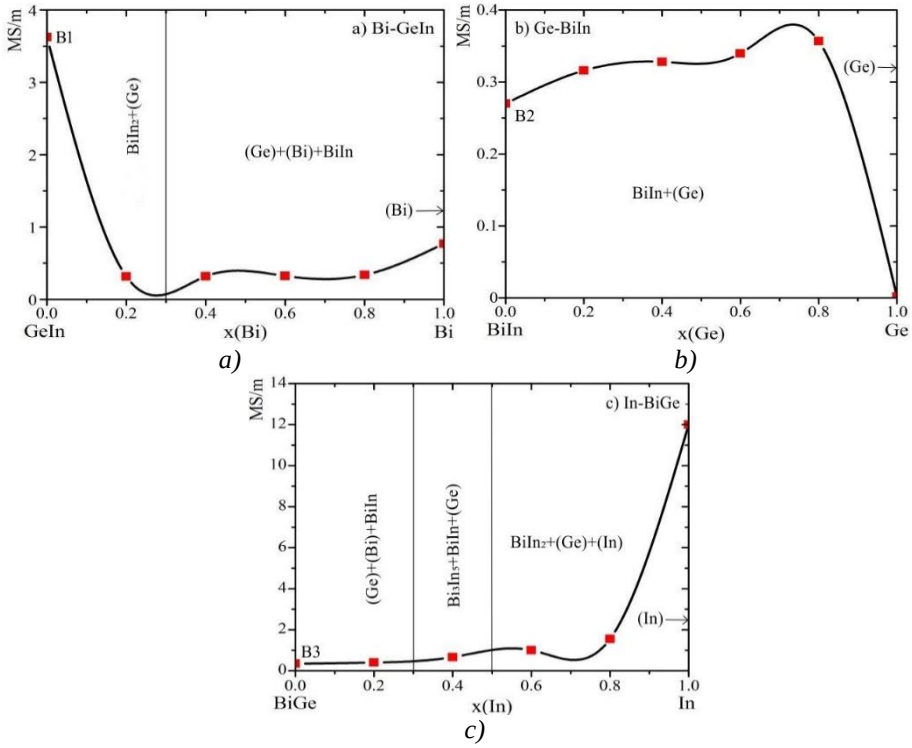

a) *b)* *c)*

Fig. 10. Graphical presentation of electrical conductivity vs. composition and phase fraction a) vertical section Bi-GeIn, b) vertical section Ge-BiIn, and c) vertical section In-BiGe.

The final equation of the predictive model in terms of Real components is:

$$Ln(\sigma + 0.10) = - 0.0125953\cdot(Bi) - 1.9440351\cdot(Ge) + 2.2392631\cdot(In) - 9.6950768\cdot(Bi)\cdot(In) + 2.8577311\cdot(Ge)\cdot(In) \quad 2$$

The repeated analysis for Natural Log model transformation confirms the significance of the Transformed Quadratic Mixture model. In this case, ANOVA confirms the adequacy of the Quadratic Mixture model (Table 8).

Table 8. ANOVA for Quadratic Mixture model.

Source	Sum of Squares	df	Mean Square	F Value	p-value Prob > F
Model	16.56761	4	4.1419	32.93354	0.000001
Linear Mixture	10.58847	2	5.2942	42.09611	0.000002
AC	5.79625	1	5.7962	46.08778	0.000013
BC	0.50360	1	0.5036	4.00429	0.066712
Residual	1.63495	13	0.1258		
Cor Total	18.20256	17			

The F-value of the Model is 32.93 and it implies that the model is significant. R-squared and other statistics after the ANOVA have good values, which confirm the justification of the choice of the adopted mathematical model (Table 9).

Table 9. R-squared and other statistics after the ANOVA.

Std. Dev.	0.35463	R-Squared	0.91018
Mean	-0.41859	Adj R-Squared	0.88254
C.V. %	84.72114	Pred R-Squared	0.72134
PRESS	5.07231	Adeq Precision	22.38151

The diagnosis of the statistical properties shows that the distribution of residuals is normal. The value of λ is 0.0, the optimum value of λ is -0.14 and the 95% confidence interval for λ (Low C.I.=-0.42, High C.I.=0.13) contains the value 0.0, thus proving the justification of the model transformation (Figure 11).

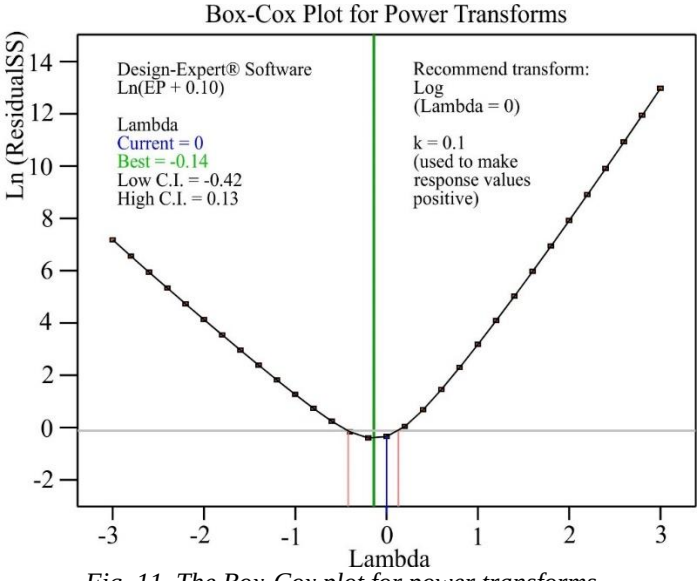

Fig. 11. The Box-Cox plot for power transforms.

Iso-lines contour plot for Electrical conductivity of Bi-Ge-In alloys defined by equation 1 is shown in Fig. 12.

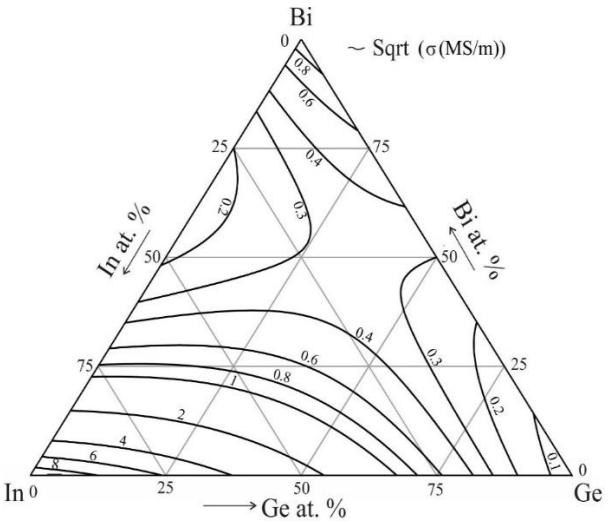

Fig. 12. Calculated iso-lines of Electrical conductivity in the ternary Bi-Ge-In system with R^2 =0.91.

Conclusion

The ternary Bi-Ge-In system has been experimentally investigated by using appropriate experimental techniques. The EDS results were matched to the calculated isothermal sections at 200 °C and 300 °C, and a close agreement was observed. The existence of a ternary compound was not detected in the tested ternary samples. On the same alloy samples, microstructural, hardness, and electrical conductivity tests were performed. Experimentally determined phases by XRD analysis were compared with the calculated isothermal section at 25 °C, and agreement between the results was reached. By using ANOVA analysis and the experimentally obtained Brinell hardness and electrical conductivity values, an appropriate mathematical model was suggested to calculate properties along with each composition range.

Acknowledgments

This work has been supported by the National Natu+32re Science Foundation of China (Project No.51950410600) and the Ministry of Education, Science and Technological Development of the Republic of Serbia (Grant No. OI172037).

References

[1] A. Djordjević, D. Minić, M. Premović, D. Manasijević, V. Ćosović: JPED, 40 (4) (2019) 623-637.

[2] W. Cao, S. L. Chen, F. Zhang, K. Wu, Y. Yang, Y. A. Chang, R. Schmid-Fetzer, W. A. Oates: Calphad, 33(2) (2009) 328–342.

[3] G. W. Burr, B. N. Kurdi, J. C. Scott, C. H. Lam, K. Gopalakrishnan, R.S. Shenoy: IBM J Res Dev, 52(4-5) (2008) 449–464.

[4] T. C. Chong, X. Hu, L. P. Shi, P. K. Tan, X. S. Miao, R. Zhao: Jpn. J Appl Phys, 42 (2B) (2003) 824–827.

[5] J. Solis, C.N. Afonso, J.F. Trull, and M.C. Morilla: J Appl Phys, 75 (12) (1994) 7788–7793.
[6] S. Raoux and T.J. Ibm, Phase Change Memory (PCM) Materials and Devices Y. Nishi, Ed., 2nd ed., Advances in Nonvolatile Memory and Storage Technology, 2014, 161–199.
[7] T. Siegrist, P. Jost, H. Volker, M. Woda, P. Merkelbach, C. Schlockermann, M. Wuttig: Nat Mater, 10 (2011) 202–208.
[8] N. Yamada, E. Ohno, N. Akahira, K. Nishiuchi, K. Nagata, M. Takao: Jpn J Appl Phys, 26 (1987) 61–66.
[9] M. Premović, D. Minić, V. Cosović, D. Manasijević, D. Živković: Metall Mater Trans A, 45A (2014) 4829-4841.
[10] D. Milisavljević, D. Minić, M. Premović, D. Manasijević, V. Ćosović, N. Košanin: Int J Thermophys, 40 (3) (2019) 29-42.
[11] C. Sinn-wen, H. Yohanes, G. Wojciech, W. Chao-hong, L. Shi-ting: Calphad, 68 (2020) 101744.
[12] R. Novakovic, E. Ricci, D. Giuranno, T. Lanata, S. Amore: Calphad, 33 (2009) 69–75.
[13] V.T. Witusiewicz, U. Hecht, B. Böttger, S. Rex: J Alloys Compounds, 428 (2007) 115–124.
[14] D. Boa, I. Ansara: Thermochim Acta, 314 (1998) 79-86.
[15] P. Y. Chevalier: Thermochim Acta, 155 (1989) 227-240.
[16] P. Y. Chevalier: Thermochim Acta, 132 (1988) 111–116.
[17] A. S. Cooper: Acta Cryst, 15 (1962) 578-582.
[18] P. Cucka, C. S. Barrett: Acta Cryst, 15 (1962) 865-875.
[19] http://periodictable.com/Properties/A/BrinellHardness.al.html, access 29.11.2018
[20] M. J. Anderson, P. J. Whitcomb, RSM Simplified, Optimizing Processes Using Response Surface Methods for Design of Experiments, Second Edition, CRC Press, Taylot & Francis Group, 2017.
[21] G. E. P. Box, N. R. Draper, Response Surfaces, Mixtures, and Ridge Analyses, Second Edition, Wiley, 2007.
[22] Stat-Ease, Handbook for Experimenters, Version 11.00, Stat-Ease, Inc. 2018.
[23] D. C. Montgomery, Design and Analysis of Experiments, Ninth Edition, Wiley, 2017.
[24] R. H. Myers, D. C. Mongomery, C. M. Anderson-Cook, Response Surface Methodology, Process and Product Optimization Using Designed Experiments, Fourth Edition, Wiley, 2016.
[25] http://periodictable.com/Properties/A/ElectricalConductivity.an.html, access 25.12.2018.